

NUMERICAL ANALYSIS OF ADAPTIVE CONTROL IN LP TURBINES

PIOTR LAMPART¹ AND ROMUALD PUZYREWSKI²

¹*The Szewalski Institute of Fluid Flow Machinery,
Fiszera 14, 80-952 Gdansk, Poland
lampart@imp.gda.pl*

²*Department of Mechanical Engineering,
Technical University of Gdansk,
Narutowicza 11/12, 80-952 Gdansk, Poland
rpuzyrew@pg.gda.pl*

(Received 9 November 2004; revised manuscript received 21 January 2005)

Abstract: A new design idea of adaptive control in LP steam turbines under conditions of (1) extraction of steam to the extraction point and (2) seasonal changes of pressure in the condenser is described in the paper. Nozzle blades of a stage located directly downstream of the extraction point or of the exit stage located upstream of the exit diffuser have adjustable trailing edges that can adapt the geometry of the blading system to changing flow conditions. The idea is validated numerically on a group of two exit stages of an extraction/condensation turbine of power 60MW. A series of flow calculations are made using a code FlowER for solving the flow of compressible viscous gas in a 3D turbomachinery environment. As a result of calculations, characteristics of the design, including the mass flow rate, flow angles in characteristic sections, enthalpy losses and turbine power are obtained in a range of given pressure drops and nozzle blade stagger angles. The adequate position of the nozzle blade is found based on these characteristics. Advantages of adaptive control in the form of increase of turbine efficiency and power are also estimated.

Keywords: LP turbine, adaptive stage, CFD

1. Introduction: the idea of adaptive control

Cogeneration of electric energy and heat in heat and power turbines requires application of adaptive control to adapt them to variable operating conditions. The main element of adaptive control is the so-called adaptive stage (AS) of flexible geometry located directly downstream of the extraction point. This flexible geometry enables reduction of the mass flow rate in the blading system without a reduction of pressure drop and without a significant increase of enthalpy losses. Thus, the full available pressure drop is used in the blading system. Expansions beyond the blading system, involving a loss of turbine power and giving rise to uncertainty in operation of the exit diffuser, are avoided.

In a typical design of adaptive stage, widely used by turbine manufacturers like LMZ and ABB-Zamech, the nozzles have movable leading edges blocking part of the blade-to-blade passage if necessary, thus reducing the mass flow rate (see the left hand side, A, of Figure 1 [1]). The mechanical construction of this stage with the so-called throttling nozzles is relatively simple, but its flow efficiency is low, both at full and low openings of the flow channel. At full opening, this is due to a low pitch-to-chord ratio, as the section of the leading edge should be able to block the entire blade-to-blade passage. At low levels of opening, a massive separation of the flow can be expected downstream of the leading edge corner. The transport of vorticity from this separation through the nozzles, and especially through the rotating blade row downstream, results in high unsteady components of forces acting on the blades of the adaptive stage.

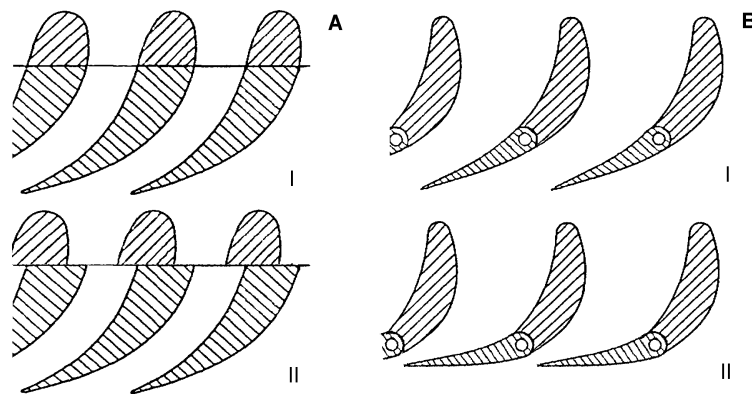


Figure 1. Nozzles with movable leading edges (throttling nozzles, A) and nozzles with rotated trailing edges (flap nozzles, B): I – nozzles fully open, II – nozzles partly open/closed

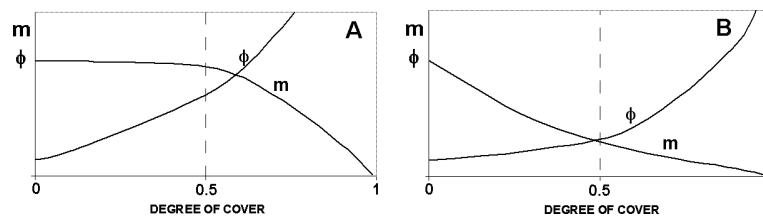


Figure 2. Mass flow rate and flow loss versus degree of cover for throttling nozzles (A) and flap nozzles (B)

Another idea of adaptive stage with movable (rotated) trailing edge was patented in [2]. This design is also called a flap nozzle and is presented on the right hand side, B, of Figure 1. Compared with the design with movable leading edges, it maintains the continuity of shape of the blade profile even at very low levels of opening. An adaptive stage with flap nozzles was installed in a 25MW turbine at the Heat and Power Station of Łódź, alternatively to the adaptive stage with throttling nozzles. A comparison of measured efficiencies of these two types of adaptive stage is presented in [3], demonstrating that with a 50% reduction of the mass flow rate from its maximum value, the level of flow losses in the stage with flap nozzles decreases

by 50% (from 70% to 20%), compared with the same stage with throttling nozzles. Qualitatively, the change of mass flow rate, m , and the change of flow losses, φ , versus the degree of cover for throttling and flap nozzles is presented in Figure 2. For throttling nozzles, the mass flow rate remains practically unchanged until the degree of cover reaches half a blade-to-blade distance, whereas flow losses exhibit a sharp rise even for low degrees of cover. As can be seen in Figure 2, the reduction of mass flow rate by changing the stator exit angle (case B) is more efficient than by the throttling effect (case A). Paper [3] also gives estimates of forces acting on the driving arm that rotates the flap nozzles.

Another example of turbine stages operating under changing flow conditions are exit stages of LP condensation turbines. Changes of flow conditions are caused here by seasonal variations of pressure in the condenser. Therefore, flow characteristics of exit stages are usually made not for one particular operating point (nominal load) but for a wide range of operating conditions. Away from the nominal point, the stage efficiency decreases as a result of increase in cascade losses and exit energy (the exit energy increases mainly due to the off-design outflow from the rotor), see *e.g.* [4, 5]. With no adaptive control, during a decrease in the condenser pressure one can expect further expansion to that pressure beyond the blading system. During an increase in the condenser pressure, the pressure behind the last stage will increase resulting in a decrease in specific volume of steam. Part of the blade-to-blade passage at the exit (even as much as half the blade height, depending on the level of pressure increase) will be blocked by a separation zone. The mass flow rate through the blade-to-blade passages will be decreased, its surplus possibly partly accommodated by leakage flows. Most likely, off-design conditions will propagate on stages located upstream. The idea of adaptive control based on flap nozzles can be adapted not only to the case of extraction of steam to the extraction point but also to the case of changing condenser pressure. The expected outcome of adaptive control is here to relieve LP turbine stages, located upstream of the last stage, of the effect of increase in the condenser pressure, and in the case of pressure decrease to assure that the blading system of the last stage consumes the full available pressure drop in the most efficient way.

The aim of this paper is to validate numerically the advantages of adaptive control in LP turbines based on the idea of adaptive stage with flap nozzles. The operation of the adaptive stage under conditions of extraction of steam to the extraction point and in the case of increase or decrease of the condenser pressure is investigated. An increase of turbine efficiency and power coming from adaptive control is estimated for a group of two exit stages of an extraction/condensation turbine of power 60MW. The calculations are made with the help of a computer code FlowER – a 3D RANS solver of turbomachinery flows. In order to simplify the process of varying the nozzle geometry, the stator blade stagger angle is varied, that is the entire stator blade is rotated rather than its trailing edge only. It is believed that this solution represents the idea of adaptive control by means of flap nozzles, as it preserves the continuity of the blade profile and consists in varying stator throats according to changes of mass flow rate in the blade-to-blade passage or downstream pressure.

2. The flow model

A series of flow computations for this paper are carried out with the help of a computer code FlowER [6]. The turbulent flow of compressible viscous gas is modelled by 3D RANS equations with the perfect gas equation. Turbulence effects are modelled using the k - ω SST model [7]. Discretisation of governing equations is made by the finite volume method. A numerical scheme of second-order accuracy in time and space is used. This is an upwind scheme of Godunov type with an ENO formula for the calculation of convective fluxes. To accelerate the process of convergence an implicit operator δ of Beam-Warming is used. The calculations are carried out in one blade-to-blade passage of the stator and rotor on an H-type grid refined near the endwalls, blade walls ($y^+ = 1-2$), leading and trailing edges. Typically 12–16 points are used in the boundary layer. The total number of grid points per one blade-to-blade passage (of a single blade row) exceeds 400 000 (92 axially \times 76 radially \times 60 circumferentially). The calculations converge to a steady state. A mixing plane approach is used to treat the relative motion of the stator and rotor, based on circumferential averaging of flow parameters in the axial gaps between the blade rows. The calculation domain also extends on the radial gaps above the rotor blades. The assumed boundary conditions are typical for turbomachinery calculations, including no slip and zero heat flux at the walls, as well as spatial periodicity at the borders of the flow channel. The pressure drop across the stage (stage group) is imposed. Therefore, for a given flow geometry, the mass flow rate is resultant. The mathematical model and numerical methods used in the solver are described in detail in [8–10]. The solver was extensively validated on real and model turbines (see [11, 12]).

3. The object of study: a group of two stages from an LP turbine

The idea of adaptive control is validated on a group of two exit stages of an extraction/condensation turbine of power 60MW – both stages have unshrouded twisted rotor blades of height 450mm and 560mm, respectively. Figure 3 shows the geometry of the investigated object in the form of flow path geometry for the LP part of the turbine (Figure 3a), computational grid in meridional and blade-to-blade sections for the group of two exit stages (Figure 3b), as well as hub-to-tip blade sections of the two exit stages (Figure 3c). Thermodynamic data for nominal operating conditions of the stage group, including the inlet static pressure, inlet static temperature, exit static pressure, exit dryness fraction and mass flow rate are given in Table 1. For the computations, a uniform distribution of total parameters is assumed at the inlet, whereas the span-wise distribution of static pressure at the exit is found from the momentum equation in the radial direction. The aim of this chapter is to investigate the flow features in the two exit stages for the nominal load, and also for a range of

Table 1. Thermodynamic data for 3D flow computations of the two-stage group

	p_0 [bar]	T_0 [°C]	p_2 [bar]	x_2 [-]	G [kg/s]
stage $L-1$	0.39	87	0.19	1.00	35.6
stage L	0.19	59	0.10	0.96	35.6

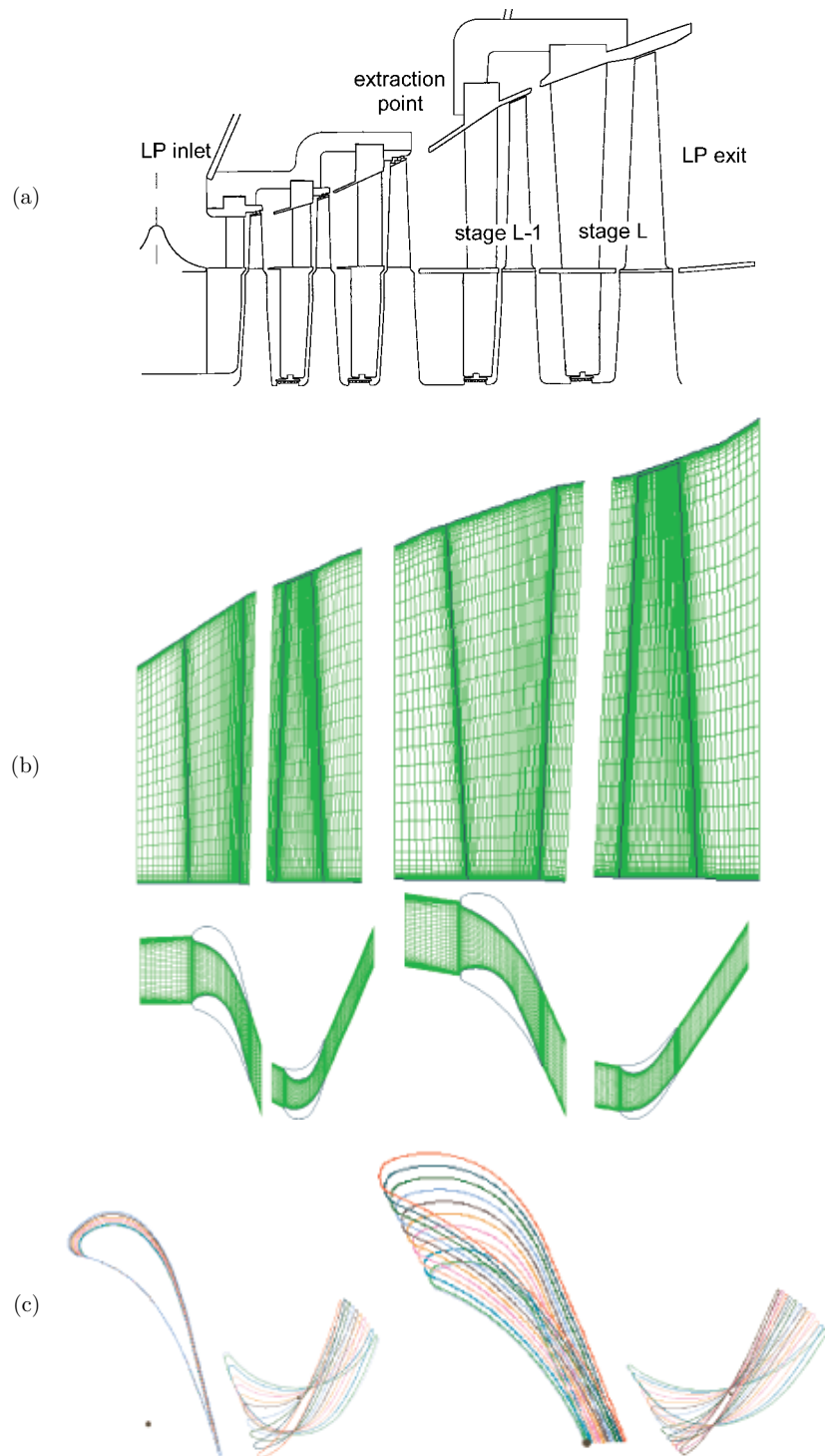


Figure 3. (a) Flow geometry of the LP part of a 60MW steam turbine; (b) computational grid for two LP turbine stages in meridional view (top) and at mid-span blade-to-blade section (bottom); (c) hub-to-tip blade sections for two LP turbine stages

operating conditions by varying the exit pressure, p_2 , between 0.15bar and 0.3bar in the last-but-one stage ($L-1$), between 0.06bar and 0.14bar in the last stage (L), and varying the exit dryness fraction for the last stage in the range of x_2 from 0.945 to 0.96.

Figure 4 shows the distribution of pressure and swirl angle due to the circumferential velocity (the swirl angle is plotted in the rotating reference frame) in the axial gap between the stators and rotors of the two investigated stages. The distribution of pressure downstream of the stator is decisive for the span-wise distribution of stage reaction, whereas the distribution of swirl angle determines inlet conditions for operation of the subsequent rotor blades. A large span-wise gradient of pressure typical for LP exit stages is apparent in the figure, which means a large gradient of reaction and significant changes in flow patterns from hub to tip. The large gradient of swirl angle (over a wide range of load the swirl angle changes virtually by 90° from hub to tip) is accommodated by the rotor blade twist, save for the hub sections where the incidence angle at the rotor blade is largely off-design (moved towards the pressure surface, compare Figure 3c). Changes in flow patterns can be observed from colour plots of Mach number in the stators and rotors at the hub, mid-span and tip presented in Figure 5 for the nominal load. The shape of Mach number contours shows the location of regions of subsonic and supersonic flow. Supersonic flow can be observed at the hub and mid-span in the stators, and at the tip in the rotors. A large separation zone can be seen near the suction surface at the rotor hub of the last stage. Figure 6 shows Mach number contours for a low and a high load away from the nominal conditions. It is clear from the figure that the conditions for expansion deteriorate at the rotor hub with the decreasing load (separation zone extends at the pressure surface of stage $L-1$ and at the rear part of the suction surface in stage L). With the increasing load, the Mach number in the stator throats increases, showing a configuration of oblique shock waves near the trailing edge of stage L . A shock wave also appears at the inlet to the rotor of stage L . Its interaction with the boundary

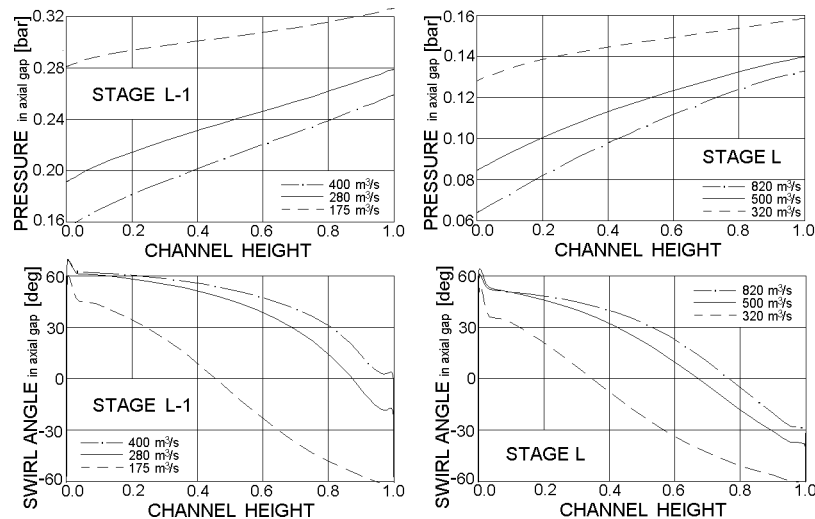


Figure 4. Span-wise distribution of static pressure (top) and swirl angle (bottom) downstream of the stator of stage $L-1$ (left) and stage L (right) for three values of load

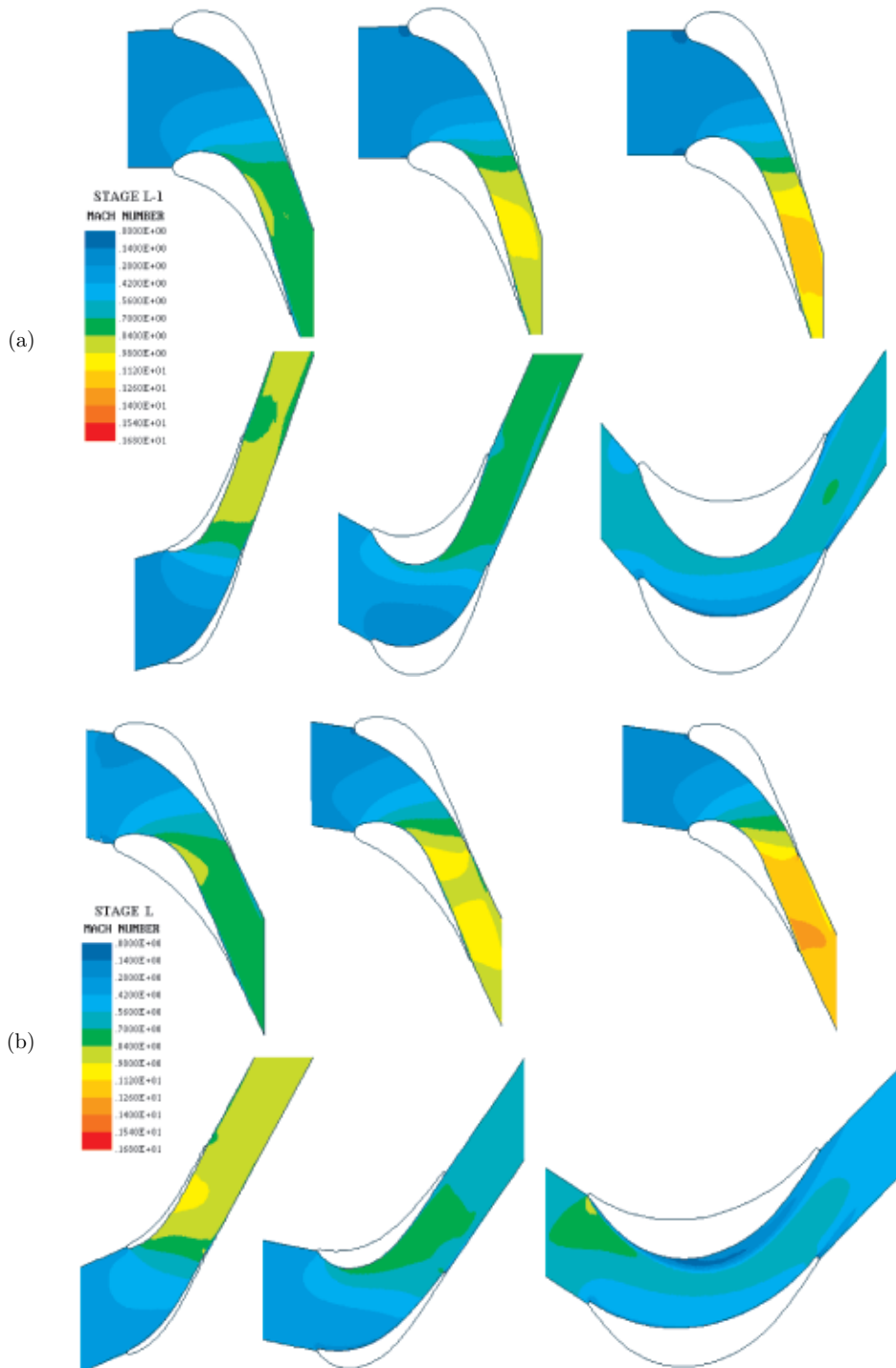


Figure 5. Mach number contours in the stator (top) and rotor (bottom) at the tip (left), mid-span (centre) and hub (right) for the nominal load:
 (a) stage *L-1* (mass flow rate 35.6kg/s, volumetric flow rate 280m³/s);
 (b) stage *L* (mass flow rate 35.6kg/s, volumetric flow rate 500m³/s)

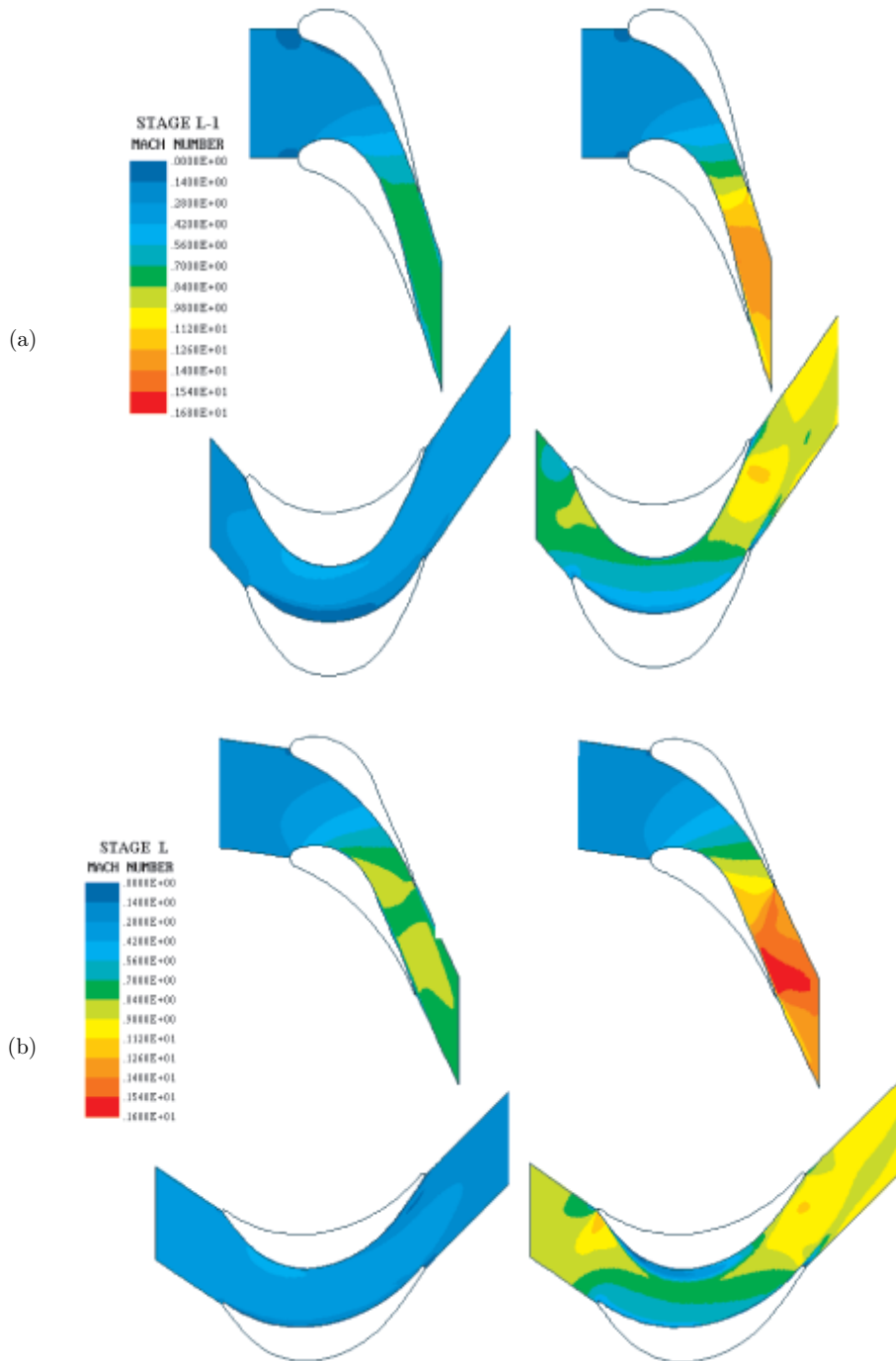


Figure 6. Mach number contours in the stator (top) and rotor (bottom) at the hub of:
 (a) stage *L-1* for a low load (mass flow rate 31.2kg/s, volumetric flow rate 175m³/s – left)
 and for a high load (mass flow rate 36.1kg/s, volumetric flow rate 400m³/s – right);
 (b) stage *L* for a low load (mass flow rate 32.1kg/s, volumetric flow rate 330m³/s – left)
 and for a high load (mass flow rate 36.3kg/s, volumetric flow rate 810m³/s – right)

layer gives rise to separation on the suction surface. Shock waves also appear near the trailing edge of the second rotor, practically along the entire blade span.

The observed phenomena have an effect on the distribution of enthalpy losses in the investigated stages¹ (see the upper row of Figure 7 showing the span-wise distribution of stage losses not including the leaving energy). Increased losses are observed in the tip region and near the hub. Both the stator and rotor contribute to these losses. The loss increase at the stator results from increased boundary layer losses and increased supersonic flow losses at the hub. In the rotor, the loss increase at low loads is due to a low reaction and separation at the hub, especially in the last stage. For high loads, the loss increase is due to increased supersonic flow losses and shock wave interactions (stage L). A detailed study of loss mechanisms in turbines can be found in [13]. Another interesting feature is the effect of leaving energy on the overall loss coefficient of the last stage. Figure 8 shows the span-wise distribution of velocity and swirl angle downstream of the rotor (in the absolute reference frame). The exit velocity is the lowest for the nominal load. For low loads, the increase in the exit velocity is due to a highly non-axial outflow from the rotor - the swirl angle reaches as much as 60° . The contribution of leaving energy to the overall enthalpy loss of the last stage is dominating, practically in the entire range of load. It is especially conspicuous for low loads, see the lower row of Figure 7 showing the span-wise distribution of stage losses with the leaving energy. The leaving energy is a direct source of loss for the last stage. The leaving energy from stage $L-1$ is used in stage L , but the non-axial outflow from the last-but-one stage is likely to increase cascade losses for the last stage. One way to reduce cascade losses due to the span-wise gradient of reaction and to decrease the leaving energy in LP turbines is optimisation of 3D blading, including compound lean and sweep of stator blades, which is described in [14, 15].

Changes of the stage reaction, swirl angle downstream of the stator (in the rotating reference frame) and rotor (in the fixed reference frame), enthalpy losses in the stator, rotor and stage (without and/or with the leaving energy) as a function of volumetric flow rate for stage $L-1$ and L are presented in Figures 9 and 10. The stage reaction, in general, exhibits an increasing tendency with the increasing load, except for the reaction at the hub for low loads. The reaction at the hub in stage L is negative almost for the entire range of load, however, it does not drop further below its value for the nominal load. The average difference between the reaction at the hub and tip is 40%–50% in stage $L-1$ and 60%–70% in stage L . The mean swirl angle in the axial gap between the stator and rotor changes by 40° – 50° in the investigated range of load, which means that there is a change of incidence at the rotor blade with changing load. The range of mean exit swirl angle is very wide, up to 90° . The mean exit swirl angle crosses the axis of 0° for the nominal load in stage $L-1$ and for some load slightly above the nominal load in stage L ($600\text{m}^3/\text{s}$ – $650\text{m}^3/\text{s}$). Changes of enthalpy losses in the

1. The enthalpy losses in a turbine stage (stage group) are defined as:

$$\zeta = \frac{i_{\text{ex}} - i_{\text{ex, is}}}{i_{\text{in}}^* - i_{\text{ex, is}}}; \quad \zeta^* = \frac{i_{\text{ex}} - i_{\text{ex, is}} + \frac{1}{2}c_{\text{ex}}^2}{i_{\text{in}}^* - i_{\text{ex, is}}},$$

where ζ , ζ^* are enthalpy losses without or with the leaving energy, respectively; c_{ex} – exit velocity, i_{in}^* , i_{ex} , $i_{\text{ex, is}}$ – inlet total enthalpy, exit static enthalpy and exit isentropic enthalpy referring to the exit pressure.

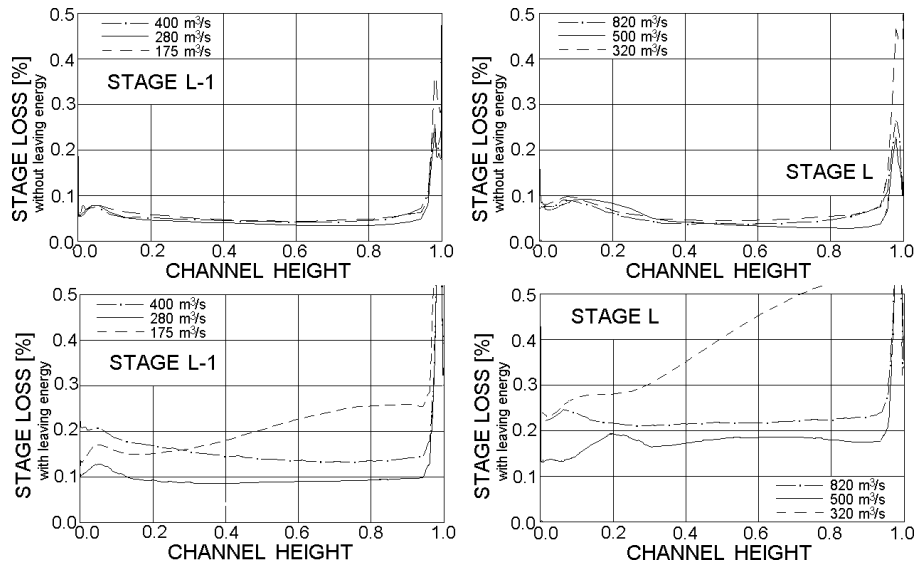


Figure 7. Span-wise distribution of enthalpy losses without (top) and with (bottom) leaving energy in stage $L-1$ (left) and stage L (right) for three values of load

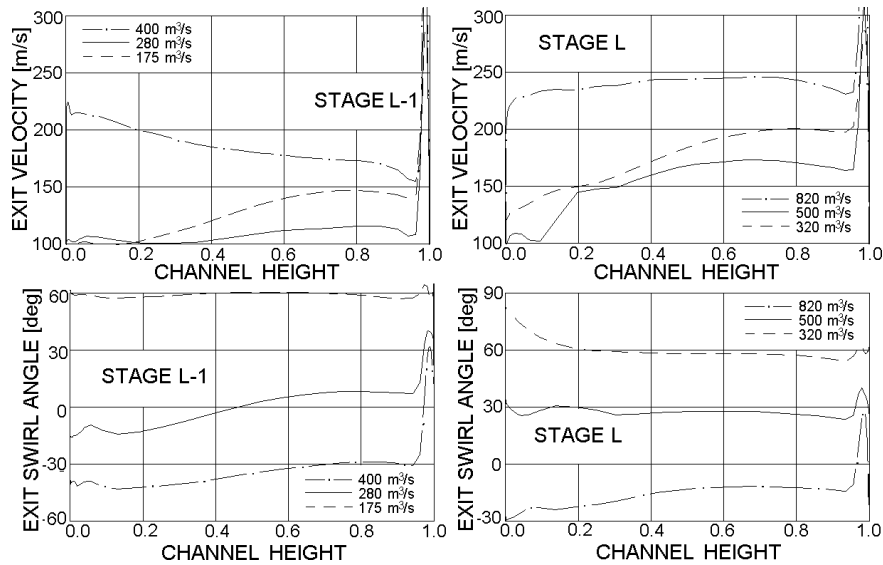


Figure 8. Span-wise distribution of velocity (top) and swirl angle (bottom) downstream of the rotor of stage $L-1$ (left) and stage L (right) for three values of load

stator with the change of load are not very significant. Enthalpy losses in the rotor and stage without the leaving energy have minimum values around the nominal load. In turn, the minimum of enthalpy losses with the leaving energy appears for the nominal load in stage $L-1$, and is slightly moved towards higher loads in stage L , where the direction of outflow from the rotor is closer to the axial direction. As can be seen from Figures 9 and 10, the flow efficiency strongly depends on the stage load, especially sharply decreasing with the decreasing load. Note that for low loads below $400\text{m}^3/\text{s}$, the characteristics of stage L (Figure 10) can be charged with considerable errors due

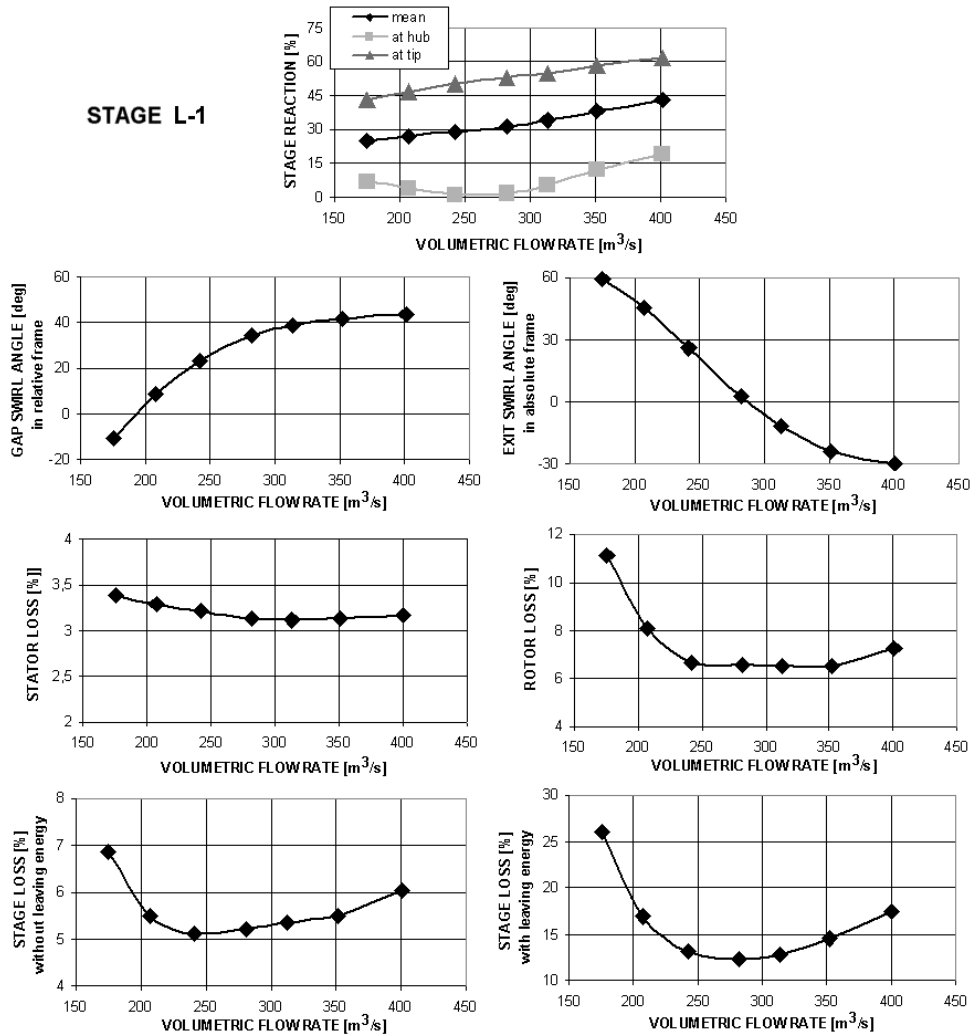


Figure 9. Stage *L-1* – change of stage reaction, swirl angle behind the stator and rotor, enthalpy losses in the stator, rotor and stage (without and with the leaving energy) as a function of volumetric flow rate

to large separation zones inside and at the exit from the computational domain. Note also that the calculations are based on the assumption of circumferential symmetry (calculations in one blade-to-blade passage of the stator and rotor), and do not take into account the effect of non-axisymmetrical flow in the exhaust hood, which may be especially important for stage *L*.

Investigations of the effects of adaptive control are carried out in two steps. In the first step, a single LP exit stage with adaptive nozzles (denoted as stage *L*) is adapted to variable operating conditions both due to extraction of steam and variation of pressure in the condenser. It is assumed that this stage is located directly downstream of the extraction point and upstream of the exit diffuser. Note that this is not the configuration presented in Figure 3a. However, this configuration is also often

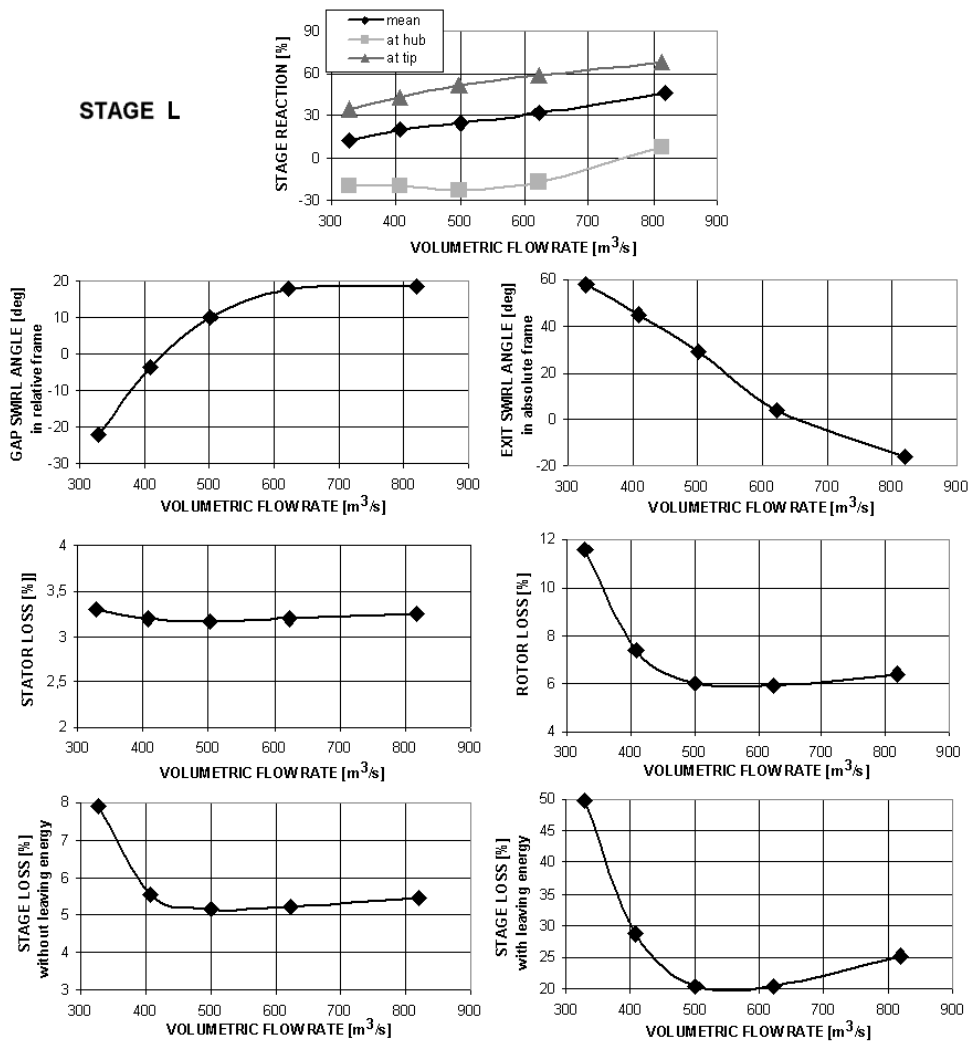


Figure 10. Stage *L* – change of stage reaction, swirl angle behind the stator and rotor, enthalpy losses in the stator, rotor and stage (without and with the leaving energy) as a function of volumetric flow rate

encountered in extraction/condensation turbines such as a 30MW turbine presented in Figure 11. Another point is that it is easier to begin the investigations of the effects of adaptive control for a single stage before moving on to the multi-stage configuration. In the second step, a group of two exit stages in the original configuration as presented in Figure 3a, with the first stage of the group (stage *L*-1) assumed to have adaptive nozzles, is adapted to the case of steam extraction.

Basically, the performance of adaptive stage based on the idea of flap nozzles is investigated. However, in order to simplify the process of varying the nozzle geometry, the stator blade stagger angle is varied, that is the entire stator blade is rotated, not only its trailing edge. The effects produced by these two solutions are certainly not identical. The distribution of stator blade load can look different in these two designs,

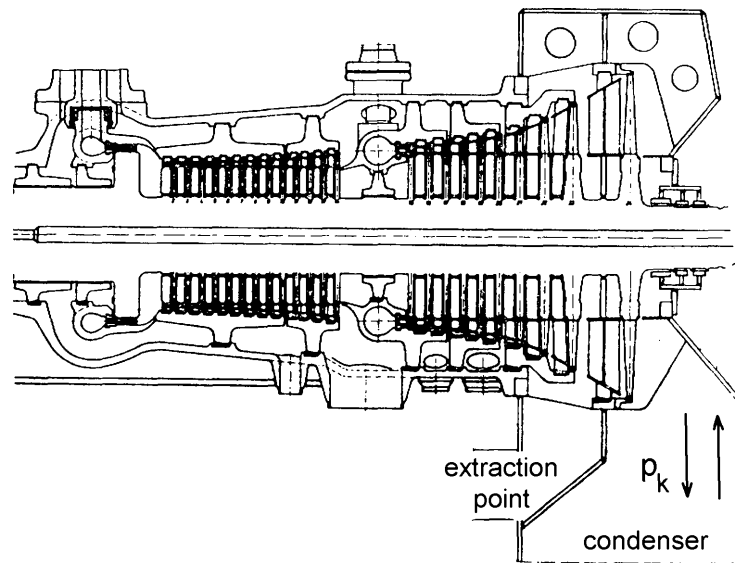


Figure 11. General view of a 30MW extraction/condensation turbine

depending on the level of throat opening. It can for example be predicted that for a low-load turbine stage, and for a decreased throat opening, the flap nozzle will be more aft-loaded. The reverse is most likely to apply in the case of increased throat opening. Minor changes in flow efficiency can also be expected. These solutions would also require different driving mechanisms to enable rotating of the nozzles, especially in view of diverging endwall contours. Anyway, both solutions are believed to represent the same idea of adaptive stage, that is preserving the continuity of the blade profile and varying stator throats according to changes of mass flow rate in the blade-to-blade passage or downstream pressure.

In the first step of investigations, a series of numerical calculations of the single LP stage geometry (stage L) are conducted in a range of change of stator blade stagger angle $\Delta\gamma = (-4^\circ, +4^\circ)$ ($\gamma = 0^\circ$ means the original nozzle geometry) and in a range of back-pressure $p_2 = 0.06\text{bar} - 0.14\text{bar}$ (inlet pressure for the stage is unchanged $p_0 = 0.19\text{bar}$, see Table 1). Based on these calculations, characteristics of the stage with rotated nozzle blades are made for the investigated range of stator blade stagger angle and stage back-pressure. These characteristics include the stage reaction, swirl angle downstream of the stator and rotor, enthalpy losses in the stage without and with the leaving energy as well as stage power as a function of stator blade geometry and mass flow rate, the latter being a quantity resulting from the computational process.

In the second step of investigations, a series of numerical calculations of the group of two LP turbine exit stages are conducted in a range of change of stage $L-1$ stator blade stagger angle $\Delta\gamma = (-3^\circ, 0^\circ)$ ($\gamma = 0^\circ$ – original nozzle geometry) and in a range of back-pressure $p_2 = 0.10\text{bar} - 0.26\text{bar}$ (downstream of the second stage; note that the inlet pressure for the stage $L-1$ is kept unchanged $p_0 = 0.39\text{bar}$, see Table 1). Then, characteristics of the stage group with rotated stage $L-1$ stator blades are made for the investigated range of stator blade stagger angle and stage back-pressure. For

the sake of reducing paper length, the presented characteristics include only changes of static pressure between the stages, stage reactions, enthalpy losses and power (for each stage and for the stage group as a whole), as a function of stage $L-1$ stator blade geometry and mass flow rate, leaving out more detailed study of incidence and outlet angles of the investigated cascades.

The analysis of the characteristics presented in subsequent chapters will show how to rotate the stator blades to adapt the stator geometry to the case of steam extraction or change of pressure in the condenser, and to raise the flow efficiency or turbine power.

4. Characteristics of a single exit stage with adaptive nozzles

The single stage characteristics are presented in Figures 12 and 13. The swirl angle downstream of the stator is given in the rotating frame of reference, whereas the swirl angle downstream of the rotor is given in the fixed reference frame. The stage power is found from the load at the rotor blades, that is $N = Mz\omega$, where M is the torsional moment due to circumferential force acting on a single blade, z – rotor blade number, ω – angular velocity. Note that values of power determined as above agree with the accuracy of $\pm 2.5\%$ with values found based on efficiency calculations, that is $N = GH(1 - \zeta)$, where G is the mass flow rate, H – isentropic enthalpy drop corresponding to the given pressure drop, ζ – enthalpy losses in the stage. Colour bold solid lines in Figures 12 and 13 link points calculated for the same nozzle geometry but for different pressure drops across the stage. Colour thin dashed lines link points calculated for the same pressure drops but for different nozzle blade stagger angles. Positive values of change of stagger angle mean opening stator throats with respect to the original geometry, negative values mean closing throats.

As can be seen from the characteristics, for a constant geometry of the stage, increasing the pressure drop across the stage is accompanied by increasing the mass flow rate, mean reaction and swirl angle in the stator-rotor gap – the incidence at the rotor blades moves further towards the pressure side of the blade. The mean rotor exit swirl angle is decreased. The reverse effects are due to a decrease in pressure drop. The enthalpy losses without or with the leaving energy have a minimum value around the nominal pressure drop. The stage power tends to increase with the increasing pressure drop and mass flow rate. For a constant pressure drop, opening stator throats causes an increase of the mean stage reaction, decrease of the mean swirl angle downstream of the stator (incidence at the rotor blades is moved towards the suction surface) and decrease of the mean exit swirl angle (which is favourable for low pressure drops but unfavourable for large pressure drops after the mean swirl angle crosses the axial direction 0°). The opposite applies to the case of closing stator throats. Enthalpy losses in the stage without the leaving energy decrease with the increased opening of stator throats for the nominal pressure drop; for low and large pressure drops they have a minimum value around the original geometry. Enthalpy losses in the stage with the leaving energy increase with the increased opening of stator throats for large pressure drops and decrease with opening throats for low pressure drops. For the nominal pressure drop they have a minimum value around the original geometry. The

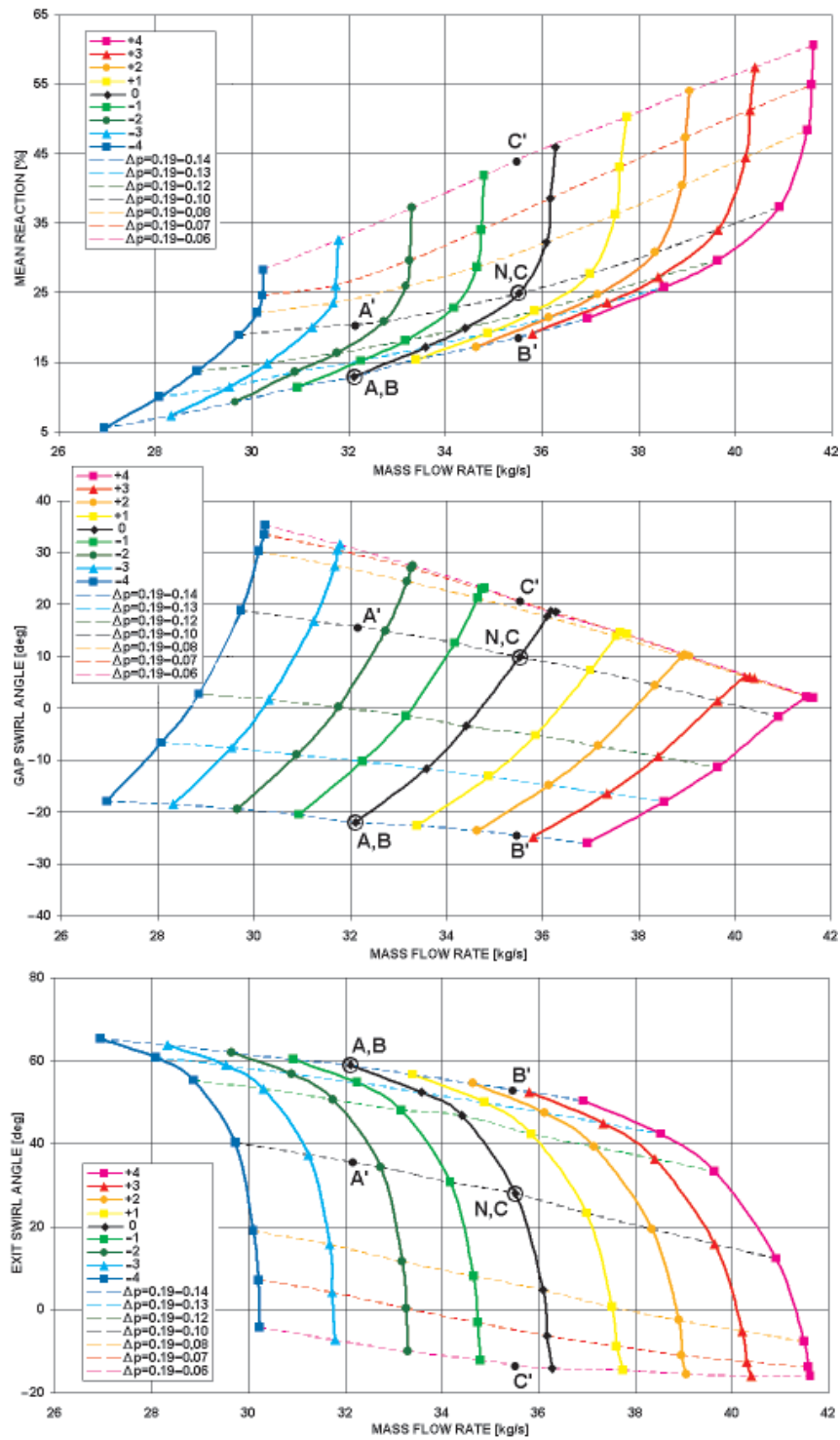


Figure 12. Stage *L* – change of stage reaction and swirl angle downstream of the stator and rotor for given values of the stator blade stagger angle as a function of mass flow rate

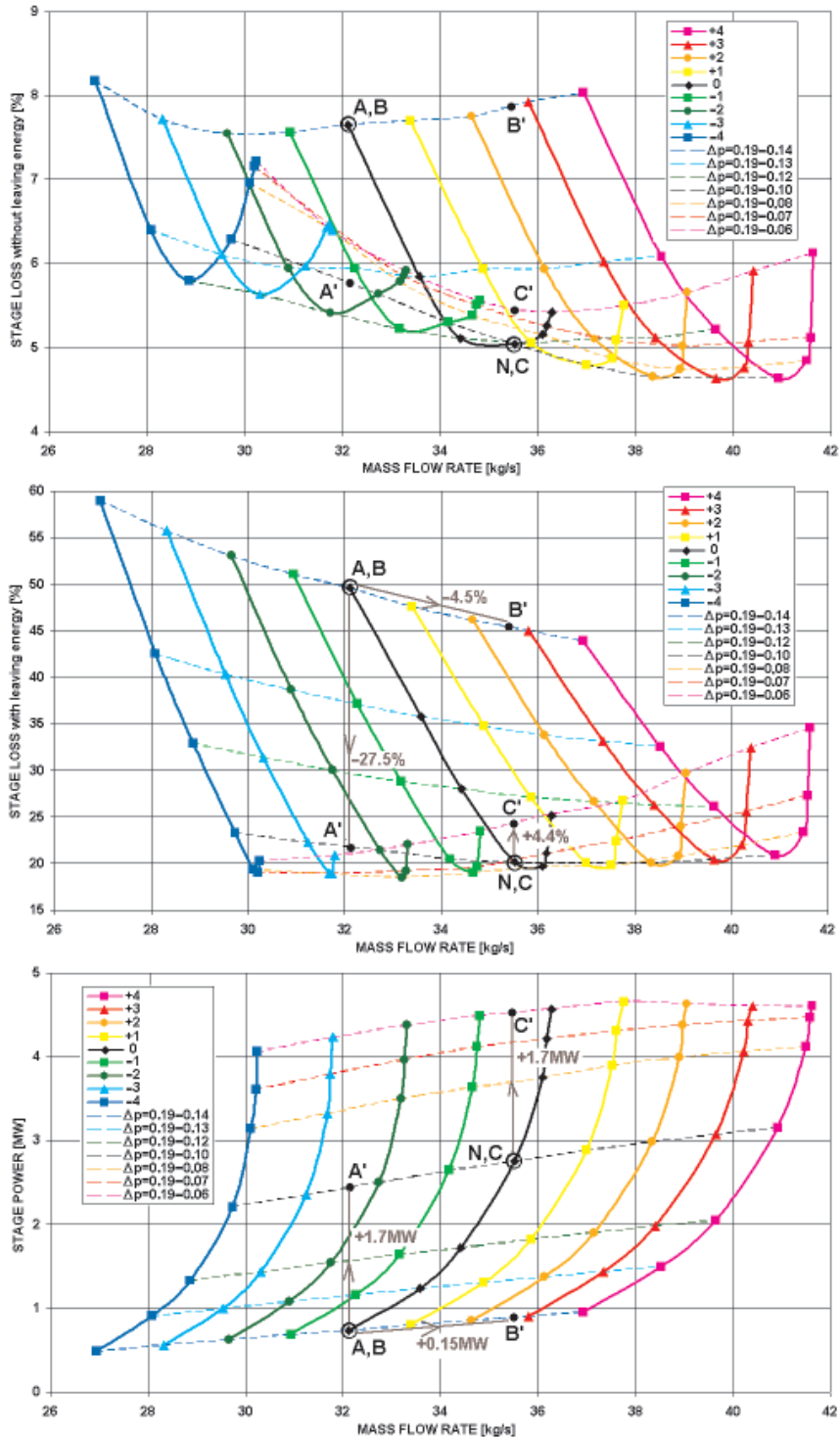


Figure 13. Stage L – change of enthalpy losses without and with the leaving energy and stage power for given values of the stator blade stagger angle as a function of mass flow rate

stage power increases with increased throat opening in the entire range of investigated pressure drops.

The following auxiliary points are indicated in Figures 12 and 13 to help estimate advantages coming from adaptive control:

- N – nominal operation of the stage;
- A – a sample point of operation under extraction of steam,
- A' – the same point after adaptive control;
- B – a sample point of operation under increase of the condenser pressure,
- B' – the same point after adaptive control;
- C – a sample point of operation under decrease of the condenser pressure,
- C' – the same point after adaptive control.

In Figure 13 (graphs of enthalpy losses with leaving energy and stage power), displacement of points of operation due to adaptive control is illustrated by grey arrows; the attached numbers indicate changes of stage losses and stage power owing to adaptive control.

5. The advantages of adaptive control in the case of steam extraction

Let us assume that upstream of the stage operating at the nominal point (mass flow rate of 35.6kg/s and pressure drop Δp from 0.19bar to 0.10bar), an additional portion of steam is extracted. Let the mass flow rate of the extracted steam be equal to 3.6kg/s. As a result of extraction, the mass flow rate in the blade-to-blade passage is reduced to 32kg/s. Without adaptive control, the pressure drop across the stage is reduced and the back-pressure is increased from 0.10bar to 0.14bar. Further expansion to the condenser pressure takes place beyond the blading system without yielding work to the rotor. The point of operation of the stage is moved in the characteristics from N to A , which is connected with an increase of enthalpy losses in the stage by about 30% to 49.5% and a decrease of stage power from 2.8MW to 0.75MW (see Figure 13).

The aim of adaptive control in the case of steam extraction is to bring part of the expansion lost for the stage back into the blading system. As can be seen from Figures 12 and 13, it can be done by closing stator throats and decreasing the stator blade stagger angle by 2.4° . Point A is then moved to point A' that lies on the line of constant pressure drop corresponding to the nominal pressure drop as before the extraction of steam. By rotating the stator blades the mean reaction is increased, incidence at the rotor blade is favourably moved towards the pressure surface, the outflow from the rotor turns favourably towards the axial direction (see Figure 12). As a consequence, cascade losses are decreased by about 2% (from 7.7% to 5.8%), whereas stage losses with the leaving energy are decreased by over 27% (from 49.5% down to 22%). In addition to that, the increased pressure drop to its nominal value results in an increased enthalpy drop and stage power, the latter increased by 1.7MW (from 0.75MW to 2.45MW), Figure 13. The stage power after adaptive control is lower by about 12% than that before steam extraction (2.8MW); practically, it is decreased only by the reduced mass flow in the blade-to-blade passage.

The increase in power obtained from adaptive control of one stage is significant not only in terms of this stage, but also in terms of the turbine as a whole, as it forms

3% of 60MW (let us recall that the investigated stage comes from a turbine of this power). Note also that by extracting more steam absolute gains in stage power from adaptive control will be even more significant since the rate of power loss along the line $N-A$ is larger than along the line $N-A'$.

6. The advantages of adaptive control in the case of change of the condenser pressure

The situation of increase and decrease of the condenser pressure will be discussed in this chapter. We will assume that any change of the condenser pressure results in a change of pressure downstream of the last stage. Let us first consider the case of pressure rise in the condenser and let the last stage operating under nominal conditions (mass flow rate 35.6kg/s, pressure drop Δp from 0.19bar to 0.10bar) experience a downstream pressure rise to $p_2 = 0.14$ bar. This pressure rise results in a decrease in specific volume of steam. Part of the blade-to-blade passage (typically at the root due to a low reaction there) can be blocked by a separation zone. For a yet higher downstream pressure, the span-wise extension of this separation zone can be significant, depending on the level of pressure increase, extending from the hub even to mid-span sections. The mass flow rate through the blade-to-blade passages is decreased and an increase in flow losses is observed. On the other hand, the mass flow rate through the stage is determined by the inlet to the LP turbine and first LP stages. Part of the mass flow rate surplus can be accommodated by leakage flows or extracted to the extraction point, but most likely, the pressure at the inlet to the last stage will rise, resulting in propagation of off-design conditions on stages located upstream. Then, the mass flow rate surplus will be lower and easier to be consumed by leakage flows or extraction points. With some degree of uncertainty we will assume that during the pressure rise in the condenser, the point of operation in the characteristics of the last stage will move from N to B (point B is here identical with point A in the case of extraction of steam to the extraction point – it is characterised by the parameters: mass flow rate 32kg/s, pressure drop Δp from 0.19bar to 0.14bar), see Figure 13. This represents a hypothetical situation, where all losses due to the back pressure rise are quantitatively assigned to the last stage, although in reality they are more evenly distributed over a group of exit stages.

We will assume that the aim of adaptive control under conditions of pressure rise in the condenser is to assure the nominal rate of mass flow through the blading system of the last stage and to exempt LP turbine stages located upstream of the last stage from off-design conditions, re-instating nominal operating conditions for those stages. As can be seen from Figures 12 and 13, this goal can be achieved by opening stator throats and turning the stator blade by 2.7° . The point of operation will then be moved along the line of new pressure drop to point B' corresponding to the nominal value of mass flow rate. As a result of turning stator blades we observe a number of counter-balance effects. First, the mean reaction is increased, second, the incidence at the rotor blade is slightly worsened, and third, the mean flow direction at the exit becomes closer to the axial direction, see Figure 12. In terms of energy effects, this results in a slight increase of cascade losses by 0.2% (from 7.7% to 7.9%), however the stage losses including the leaving energy are considerably decreased by as much

as 4.5% (from 49.5% to 45%). Moreover, the increase of mass flow rate in the blade-to-blade passage to its nominal value gives rise to an increase of stage power from 0.75MW to 0.9MW, see Figure 13. Truly, gains in stage power are not very impressive due to a low pressure drop available for this stage, however it is also important that the pressure rise in the condenser does not effect turbine stages located upstream of the last stage, which still experience nominal operating conditions. Let us note that the uncertainty of determination of the operating point in the characteristics mentioned above concerns only point B and not point B' .

Let us now consider the case of pressure drop in the condenser and assume that the last stage operating at nominal conditions faces a pressure drop to a downstream pressure of 0.06bar. With the unchanged mass flow rate determined by the inlet to the turbine, the point of operation of the last stage does not change, that is the pressure behind the stage still remains at 0.10bar and further expansion to the pressure of 0.06bar takes place beyond the blading system. The operational point connected with the situation of pressure drop in the condenser is denoted in the characteristics as C (identical with point N). In spite of an increased pressure drop available for the last stage, the stage power remains unchanged.

The aim of adaptive control in this case is to take advantage of the available increased pressure drop and prevent steam expansion beyond the blading system. It follows from Figures 12 and 13 that this goal can be achieved by closing stator throats by 0.6° . The operational point C is then moved to point C' located on the line of pressure drop Δp from 0.19bar to 0.06bar. Turning the stator blades increases the stage load. There is a significant increase of stage reaction, the incidence at the rotor blades moves further towards the pressure side, the mean exit swirl angle is moved to the other side of the 0° axis with the flow direction at the exit slightly nearer to the axial direction, see Figure 12. As a consequence, cascade losses are increased by 0.5% (from 5.0% to 5.5%), and due to an increased exit velocity, stage losses with leaving energy are increased by over 4% (from 20.1% to 24.5%). On the other hand, the increased pressure drop across the stage means an increased isentropic enthalpy drop, so finally the stage power is increased from 2.8MW to 4.5MW, see Figure 13. Gains in stage power obtained from consuming the entire available pressure drop in the blading system are remarkable in terms of the last stage itself, and remain significant in terms of power of the whole turbine.

7. Characteristics of a two stage group with adaptive nozzles

The two-stage group characteristics are presented in Figures 14 and 15. The enthalpy losses of the subsequent stages and the stage group include the effect of leaving energy. The stage (stage group) power is found from the load at the rotor blades. Colour bold solid lines in Figures 14 and 15 link points calculated for the same nozzle geometry but for different pressure drops across the stage. Colour thin dashed lines link points calculated for the same pressure drops but for different stage $L-1$ nozzle blade stagger angles. The negative values of change of the stagger angle mean closing stator throats with respect to the original geometry.

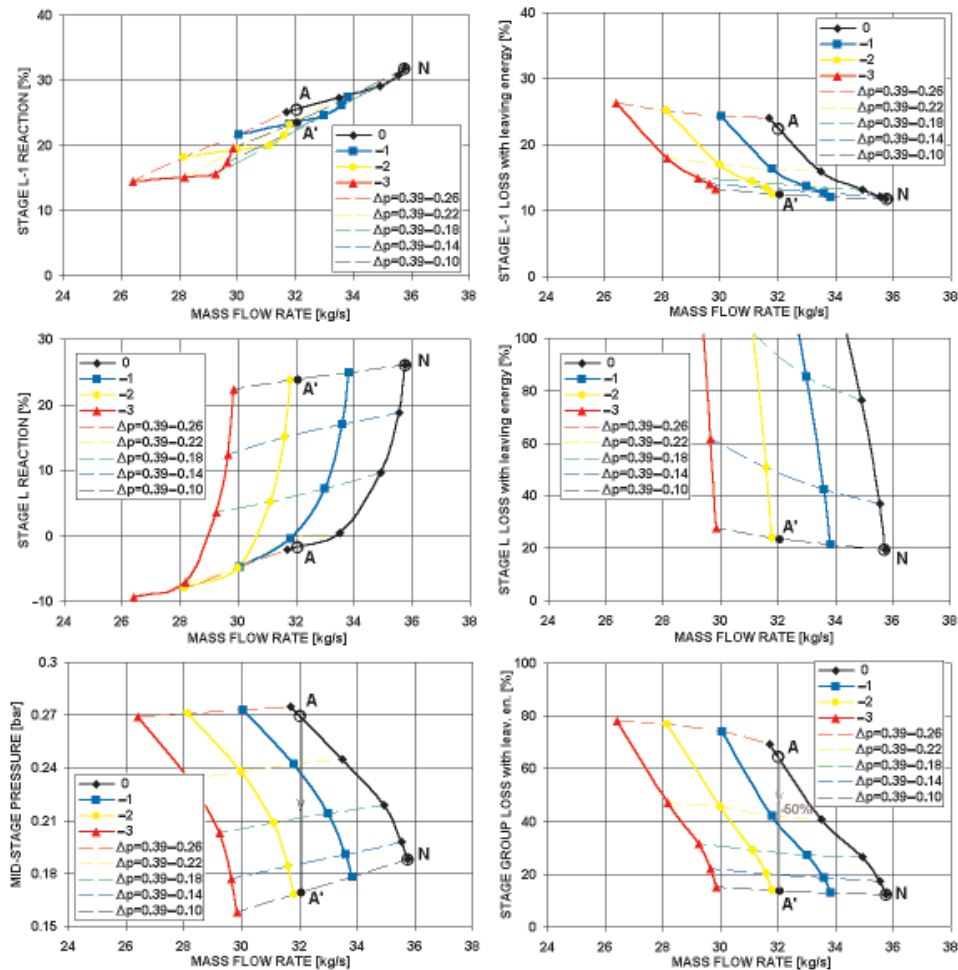


Figure 14. Change of mean reaction of stage $L-1$ and stage L , mid-stage static pressure (left column), enthalpy losses (including the leaving energy) in stage $L-1$, stage L and stage group (right column) for given values of stage $L-1$ stator blade stagger angle as a function of mass flow rate

As seen from the characteristics, decreasing the pressure drop in the stage group decreases the mass flow rate in the blading system. For a constant stage group geometry, there is a decrease in the mean reaction of each stage with the decreasing mass flow rate. Especially significant is the decrease of reaction in stage L . The mean reaction of the exit stage (stage L) drops to zero when the mass flow rate decreases by less than 2kg/s ! The calculations of the two stage group show that for the original geometry and for a fixed stage $L-1$ upstream pressure of 0.39bar , the rise of downstream pressure above 0.20bar yields negative power of the stage L . Enthalpy losses in stage L increase above 100% for the mass flow rates below 34.2kg/s . The volumetric flow rates drop there below $250\text{m}^3/\text{s}$ (compare stage L characteristics presented in Figure 10). This refers to the situation where energy must be supplied to rotate the rotor blades of this stage. In other words, extraction of steam of more than 1.5kg/s upstream of the stage group means that the second stage does not produce

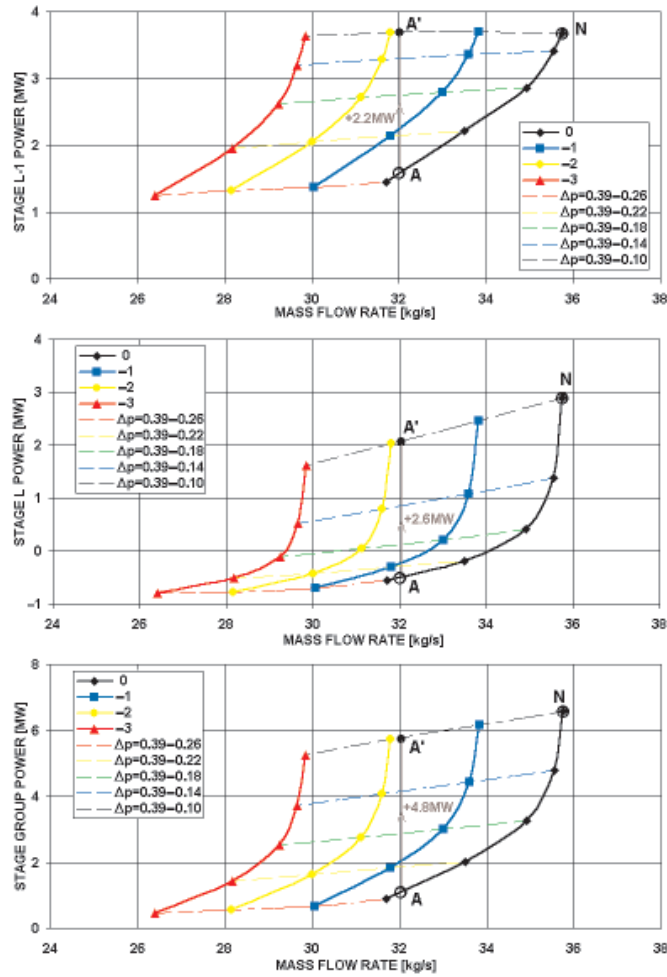


Figure 15. Change of power of stage *L*-1, stage *L* and stage group for given values of stage *L*-1 stator blade stagger angle as a function of mass flow rate

power any longer and starts consuming power generated by upstream stages. This clearly exhibits how severe the case of steam extraction is for a group of exit stages and shows the necessity of adaptive control.

Closing stage *L*-1 stator throats for a constant pressure drop causes a slight decrease of the mid-stage pressure and stage reaction for each stage. Enthalpy losses in stage *L*-1 are slightly increased with closing stage *L*-1 stator throats; an increase of enthalpy losses in stage *L* is more significant, which translates into a moderate decrease of stage group enthalpy losses with closing stage *L*-1 stator throats. The power of stage *L*-1 usually exhibits a slightly decreasing tendency with closing its stator throats. An exception is for the nominal pressure drop where a slight increase in power of stage *L*-1 is observed due to the decreased mid-stage pressure. On the other hand, there is a consecutive decrease in power of stage *L* and in power of the stage group with closing stage *L*-1 stator throats.

Similar to the characteristics presented in Figures 12 and 13, the following auxiliary points are indicated in Figures 14 and 15 to help estimate advantages coming from adaptive control:

- N – nominal operation of the stage,
- A – a sample point of operation under extraction of steam,
- A' – the same point after adaptive control.

In selected graphs of stage (stage group) losses and power in Figures 14 and 15, the displacement of points of operation due to adaptive control is illustrated by grey arrows; the attached numbers indicate changes of stage (stage group) losses and power owing to adaptive control.

8. The advantages of adaptive control in the case of steam extraction (two-stage group)

Let us assume that upstream of the stage group operating at the nominal point (mass flow rate 35.6kg/s, pressure drop Δp from 0.39bar to 0.10bar), an additional portion of steam is extracted. Let the mass flow rate of the extracted steam be equal to 3.6kg/s. As a result of this extraction, the mass flow rate in the blade-to-blade passage is reduced to 32kg/s. Without adaptive control, the pressure drop across the stage is reduced and the back-pressure is increased to 0.27bar! Further expansion to the condenser pressure takes place beyond the blading system without yielding work to the rotor. The point of operation of the stage is moved in the characteristics from N to A . This is connected with a decrease of reaction in stage $L-1$ by approximately 7% (from 32% to 25%) and by 29% in stage L (from 27% to -2%). There is an increase of enthalpy losses in stage $L-1$ by 11% (from 12% to 23%); enthalpy losses in stage L increase from 20% up to above 100%, resulting in an increase of enthalpy losses in the stage group by over 50% (from 13% to 64%). The power of stage $L-1$ is decreased from 3.7MW to 1.6MW, power of stage L is decreased from 2.8MW down to -0.5MW (negative value – stage L consumes power), resulting in the stage group power decreasing from 6.5MW to 1.1MW, see Figures 14 and 15.

As already mentioned, the aim of adaptive control in the case of steam extraction is to bring back the expansion to the blading system. As can be seen from Figures 14 and 15, this can be done by closing stage $L-1$ stator throats and decreasing the stator blade stagger angle by 1.8°. Point A is then moved to point A' that lies on the line of constant pressure drop corresponding to the nominal pressure drop (from 0.39bar to 0.10bar) as before the extraction of steam. By rotating the stage $L-1$ stator blades, the mid-stage pressure is decreased from 0.27bar to 0.17bar. The mean reaction of stage $L-1$ is further (slightly) decreased by 3%, whereas that of stage L is increased by 26% up to 24%. The enthalpy losses in stage $L-1$ are reduced by 10% to about 13% and from a value exceeding 100% down to 22% in stage L , resulting in a decrease of losses in the stage group by 50% (down to 14%). The power of stage $L-1$ is increased by 2.2MW to 3.8MW, power of stage L is increased by 2.6MW to 2.1MW, and the stage group power is increased by 4.8MW to 5.8MW, Figures 14 and 15. The stage power after adaptive control is lower by about 11% than that before the steam extraction (6.5MW) – again it is decreased practically only by the reduced mass flow rate in the blade-to-blade passage.

The increase in power obtained from adaptive control of the stage group is significant, as it forms 8% of the turbine power (60MW). Note also that due to the decreased mid-stage static pressure resulting from rotating the stage $L-1$ stator blades, the obtained value of power of stage $L-1$ exceeds the nominal value for the original geometry, even though the mass flow rate is reduced. Extracting more steam increases absolute gains in stage group power due to adaptive control as the rate of power loss along the line $N-A$ is larger than along the line $N-A'$.

It is also important to note that the results of RANS calculations of low-efficiency configurations far away from the nominal flow conditions (massive separations, reverse flows, indetermination of inlet/exit boundary conditions, that is a difficulty to establish whether a boundary is that of an inlet or exit) can be charged with considerable computational errors. Especially, the absolute values of enthalpy losses may be far from reality and need experimental verification (in fact they are not shown above 80% loss). However, it is not likely that the above mentioned uncertainties can reverse the presented tendencies and invalidate the discussed advantages of adaptive control.

9. Conclusions

Adaptive control serves as a means of increasing flexibility of the blading system under changing flow conditions. In this paper, cogeneration of electric energy and heat as well as seasonal variations of the condenser pressure were considered. The idea of adaptive control in LP turbines based on nozzles with the adjustable blade stagger angle, representing the patented concept of flap nozzles with rotated trailing edges, was validated numerically with the help of a 3D RANS solver FlowER. A series of flow calculations of the LP turbine exit stage and a group of two exit stages of a 60MW extraction/condensation turbine were made for a range of pressure drop across the stage (stage group) and stagger angle of the adaptive stage stator blade.

It was found that in the case of steam extraction, the stator blades of the adaptive stage located directly downstream of the extraction point should have their throats reduced. By means of that measure, expansion beyond the blading system is avoided and full available pressure drop is used for rotor work. The enthalpy losses in the adaptive stage and especially in downstream stages are significantly reduced. There is a significant increase in stage (stage group) power. For the investigated LP exit stage and the upstream extraction of a 10% mass flow rate, the power increase is just below 2MW. For the extraction of a 10% mass flow rate upstream of the group of two exit stages, the power increase was found to be even as high as over 2MW per stage.

In the case of rise in the condenser pressure, nozzle throats of the adaptive stage (last stage) should be open. The enthalpy losses in the stage are reduced. Gains in stage power are moderate, mainly due to maintaining the nominal mass flow rate in the blade-to-blade passages. In this case, adaptive control of the last stage prevents propagation of off-design flow conditions on upstream turbine stages. In the case of decrease in the condenser pressure, nozzle throats should be reduced. This helps to avoid expansion beyond the blading system and to take advantage of the full available pressure drop. Gains in stage power are significant, just below 2MW for the

investigated LP exit stages and a back pressure decrease from 0.10bar to 0.06bar, although in this case they take place at a slightly increased level of flow losses in the blading system.

References

- [1] Deych M E and Troyanovskii B M 1964 *Investigation of Axial Turbine Stages*, Masgiz, Moscow (in Russian)
- [2] Puzyrewski R 1978 *Cascade of Nozzles for Mass Flow Rate Control in a Heat and Power Turbine*, Polish Patent Office, No. 96981, 1978-07-05 (in Polish)
- [3] Puzyrewski R, Malec A and Gardzilewicz A 1994 *Proc. 10th Conf. Steam and Gas Turbines for Power and Cogeneration Plants*, Karlovy Vary, Czech Republic, pp. 219–223
- [4] Perycz S 1992 *Steam and Gas Turbines Series Turbomachinery*, Vol. 10, Ossolineum, Wroclaw-Warsaw-Cracow (in Polish)
- [5] Lampart P and Gardzilewicz A 1999 *Proc. Colloquium Fluid Dynamics'99*, Prague, Czech Republic, pp. 131–138
- [6] Yershov S and Rusanov A 1996 *The Application Package FlowER for the Calculation of 3D Viscous Flows through Multi-stage Turbomachinery*, Certificate of State Registration of Copyright, Ukrainian State Agency of Copyright and Related Rights, February 19 (in Ukrainian)
- [7] Menter F R 1994 *AIAA J.* **32** (8) 1598
- [8] Yershov S 1994 *Mathematical Modelling* **6** (11) 58 (in Russian)
- [9] Yershov S, Rusanov A, Gardzilewicz A, Lampart P and Świryczuk J 1998 *TASK Quart.* **2** (2) 319
- [10] Lampart P, Świryczuk J and Gardzilewicz A 2001 *TASK Quart.* **5** (2) 191
- [11] Lampart P, Yershov S and Rusanov A 2002 *Ciepłne Maszyny Przepływowe (Turbomachinery)* **122** 63
- [12] Rusanov A, Yershov S, Lampart P, Świryczuk J and Gardzilewicz A 2002 *TASK Quart.* **6** (4) 591
- [13] Denton J D 1993 *Trans. ASME – J. Turbomachinery* **115** 621
- [14] Lampart P and Yershov S 2003 *Trans. ASME – J. Engng. Gas Turbines & Power* **125** (1) 385
- [15] Lampart P 2002 *ASME Pap.* IJPGC2002-26161